Published in final edited form as:
Cancer Cell. 2014 April 14; 25(4): 501–515. doi:10.1016/j.ccr.2014.03.007.

Cancer-secreted miR-105 destroys vascular endothelial barriers to promote metastasis

Weiying Zhou[1,13], **Miranda Y. Fong**[1], **Yongfen Min**[16], **George Somlo**[2], **Liang Liu**[1,14], **Melanie R. Palomares**[2,3], **Yang Yu**[1,14], **Amy Chow**[1], **Sean Timothy Francis O'Connor**[1], **Andrew R. Chin**[1,12], **Yun Yen**[4,9], **Yafan Wang**[9], **Eric G. Marcusson**[15], **Peiguo Chu**[5], **Jun Wu**[6], **Xiwei Wu**[10], **Arthur Xuejun Li**[7], **Zhuo Li**[11], **Hanlin Gao**[1,10], **Xiubao Ren**[14], **Mark P. Boldin**[8], **Pengnian Charles Lin**[16], and **Shizhen Emily Wang**[1,*]

[1]Department of Cancer Biology, City of Hope Beckman Research Institute and Medical Center, Duarte, CA 91010, USA

[2]Department of Medical Oncology, City of Hope Beckman Research Institute and Medical Center, Duarte, CA 91010, USA

[3]Department of Population Sciences, City of Hope Beckman Research Institute and Medical Center, Duarte, CA 91010, USA

[4]Department of Molecular Pharmacology, City of Hope Beckman Research Institute and Medical Center, Duarte, CA 91010, USA

[5]Department of Pathology, City of Hope Beckman Research Institute and Medical Center, Duarte, CA 91010, USA

[6]Department of Comparative Medicine, City of Hope Beckman Research Institute and Medical Center, Duarte, CA 91010, USA

[7]Department of Information Science, City of Hope Beckman Research Institute and Medical Center, Duarte, CA 91010, USA

[8]Department of Molecular and Cellular Biology, City of Hope Beckman Research Institute and Medical Center, Duarte, CA 91010, USA

[9]Cores of Translational Research Laboratory, City of Hope Beckman Research Institute and Medical Center, Duarte, CA 91010, USA

[10]Integrative Genomics, City of Hope Beckman Research Institute and Medical Center, Duarte, CA 91010, USA

[11]Electron Microscopy, City of Hope Beckman Research Institute and Medical Center, Duarte, CA 91010, USA

[*]Correspondence: S. Emily Wang, ewang@coh.org, Department of Cancer Biology, Beckman Research Institute of City of Hope, 1500 East Duarte Road, KCRB Room 2007; Duarte, CA 91010, USA, TEL: 1-626-2564673 x63118; FAX: 1-626-3018972.

[12]City of Hope Irell & Manella Graduate School of Biological Sciences, Duarte, CA 91010, USA

[13]Department of Pharmacology, College of Pharmacy, The Third Military Medical University, Chongqing, 400038, China

[14]Department of Immunology & Biotherapy, Tianjin Cancer Hospital, Tianjin, 300060, China

[15]Oncology and Basic Mechanisms, Regulus Therapeutics, San Diego, CA 92121, USA

[16]Center for Cancer Research, National Cancer Institute, Frederick, MD 21702, USA

SUMMARY

Cancer-secreted miRNAs are emerging mediators of cancer–host crosstalk. Here we show that miR-105, which is characteristically expressed and secreted by metastatic breast cancer cells, is a potent regulator of migration through targeting the tight junction protein ZO-1. In endothelial monolayers, exosome-mediated transfer of cancer-secreted miR-105 efficiently destroys tight junctions and the integrity of these natural barriers against metastasis. Overexpression of miR-105 in non-metastatic cancer cells induces metastasis and vascular permeability in distant organs, whereas inhibition of miR-105 in highly metastatic tumors alleviates these effects. MiR-105 can be detected in the circulation at the pre-metastatic stage, and its levels in the blood and tumor are associated with ZO-1 expression and metastatic progression in early-stage breast cancer.

INTRODUCTION

Metastasis is the leading cause of mortality in cancer patients. Nearly 50% of breast cancer (BC) patients treated with chemotherapeutic and/or hormonal agents develop distant metastatic disease (Nicolini et al., 2006; Rubens, 2001); these patients face a 5-year survival rate of only ~20% (Yardley, 2010). Therefore, there is a great and urgent need to develop predictive or early diagnostic markers for metastasis and to elucidate the molecular mechanisms of metastasis that would allow development of efficient treatment options. In the “seed and soil” hypothesis for metastasis (Paget, 1889), migratory tumor cells leave the primary tumor through intravasation, disseminate throughout the body via the circulation, and eventually engraft in a distant organ that provides an appropriate microenvironment. These consecutive steps require close interplay between cancer cells and their microenvironment. Among the multiple factors underlying metastasis, the adaptation of primary tumor microenvironment and pre-/metastatic niches by cancer to facilitate cancer cell dissemination and distant engraftment plays an important pro-metastatic role that is starting to be recognized (Chambers et al., 2002; Kaplan et al., 2005; Podsypanina et al., 2008; Psaila and Lyden, 2009; Sethi and Kang, 2011). The recent discovery of microRNAs (miRNAs) and their extracellular presence suggest a potential role of these regulatory molecules in defining the metastatic potential of cancer cells and mediating the cancer–host communication.

MiRNAs are small non-coding RNAs that base-pair with the 3′ untranslated regions (UTRs) of protein-encoding mRNAs, resulting in mRNA destabilization and/or translational inhibition. The biogenesis of miRNAs is tightly controlled, and dysregulation of miRNAs is linked to cancer (Calin and Croce, 2006; Iorio et al., 2005). MiRNAs are also present

extracellularly, either through binding to protein or lipid carriers (Arroyo et al., 2011; Turchinovich et al., 2011; Vickers and Remaley, 2012) or as a major RNA component of exosomes (Redis et al., 2012; Valadi et al., 2007). Exosomes are small (30–100 nm) membrane-encapsulated vesicles that are released into the extracellular environment by many cell types, including cancer cells (Skog et al., 2008; Valadi et al., 2007; Yuan et al., 2009). Exosomal RNAs are heterogeneous in size but enriched in small RNAs, such as miRNAs. Cancer-secreted exosomes and miRNAs can be internalized by other cell types in the primary tumor microenvironment and pre-/metastatic niches (Hood et al., 2011; Peinado et al., 2012; Skog et al., 2008; Yuan et al., 2009; Zhang et al., 2010; Zhuang et al., 2012). MiRNAs loaded in these exosomes, which to a certain extent reflect the dysregulated miRNA profile in cancer cells, can thus be transferred to recipient niche cells to exert genome-wide regulation of gene expression. In addition, cancer-derived exosomal miRNAs may bind as ligands to Toll-like receptors in surrounding immune cells (Fabbri et al., 2012). Therefore, cancer-secreted miRNAs may play a crucial role in regulating various cellular components of the tumor microenvironment in order to facilitate metastasis.

Cancer-derived miRNAs have been detected in the blood of cancer patients, where their levels distinguish cancer patients from healthy controls (Mitchell et al., 2008; Taylor and Gercel-Taylor, 2008). Previous studies from us and by other groups have identified circulating miRNAs associated with the histopathological features of breast tumors and clinical outcomes in BC patients (Heneghan et al., 2010; Jung et al., 2012; Roth et al., 2010; Wu et al., 2012; Zhu et al., 2009). Some of these miRNAs may play a role in the metastatic process. The goal of this study is to identify cancer-secreted miRNAs that participate in cancer metastasis by adapting the niche cells.

RESULTS

MBC-secreted exosomal RNA regulates migration of endothelial cells

We chose the MDA-MB-231 metastatic BC (MBC) line and the MCF-10A non-cancerous mammary epithelial line as models for studying cancer-secreted exosomes and miRNAs. Exosomes purified from conditioned media (CM) by ultracentrifugation exhibited typical cup-shaped morphology by electron microscopy and a size range of 30–100 nm (Figure 1A). We focused on endothelial cells in this study for their critical barrier function during metastasis. When exosomes labeled with the fluorescent dye DiI were incubated with primary human microvascular endothelial cells (HMVECs), the recipient cells exhibited high uptake efficiency, as indicated by fluorescence microscopy (Figure 1B) and flow cytometry (Figure 1C), without a significant difference between MCF-10A- and MDA-MB-231-derived exosomes. After a 24 hr incubation with labeled exosomes, >90% of recipient cells were positive for DiI fluorescence (Figure 1C). Among a series of cellular analyses in exosome-treated HMVECs, we found that the transwell migration of endothelial cells was significantly stimulated by MDA-MB-231-secreted, but not MCF-10A-secreted exosomes (Figure 1D). Transfection of total or small RNA extracted from MDA-MB-231 exosomes, but not that from the MCF-10A exosomes, recapitulated the migration-inducing effect (Figure 1E), thereby indicating that the unique small RNA content of MDA-MB-231 exosomes functions as a migratory regulator in endothelial cells.

MiR-105 is specifically expressed and secreted by metastatic BC cells and can be transferred to endothelial cells via exosome secretion

To identify the exosome-associated small RNA(s) that induce migration, we selected and profiled all small RNAs in the exosomes by Solexa deep sequencing. Exosomes from MDA-MB-231 and MCF-10A cells exhibited similar small RNA composition (Figure S1A). We focused on miRNAs which are known for their gene regulatory function, identifying a list of miRNAs differentially secreted between the two lines (Table S1). Among these, some showed the corresponding up- or down-regulation in the cells and the exosomes whereas others exhibited opposite changes between the exosomal and cellular compartments, which may suggest cell-type-specific mechanisms for highly selective enrichment or exclusion of the miRNA in exosome-mediated secretion. We further focused on miR-105 that was predicted by multiple algorithms (TargetScan, miRDB, and PicTar) to target *TJP1* (tight junction protein 1; also known as zonula occludens 1 or ZO-1), a migration-related gene. The secretion of mature miR-105 was highly specific to MDA-MB-231 and its expression was significantly higher in these cells compared to MCF-10A (Table S1 & Figure 2A–B). Although the primary (pri-) and precursor (pre-) miR-105 also exhibited higher intracellular levels in MDA-MB-231, these forms were not detectable in exosomes (Figure S1B–C). Among a panel of BC lines, the expression and secretion of miR-105 were specific to highly metastatic cells originally isolated from pleural effusion (Figure 2A–B).

To confirm that MBC-secreted miR-105 can be transferred to endothelial cells via exosomes, we measured the miR-105 levels in HMVECs treated with exosomes derived from MCF-10A or MDA-MB-231 cells. An increase of the cellular level of mature miR-105, but not pri- or pre-miR-105, was observed in recipient HMVECs following the treatment with MBC-originated exosomes with kinetics starting at 4 hr and peaking at 24 hr (Figure 2C–D), similar to that observed for exosome uptake (Figure 1C). We conclude that this increase of miR-105 reflects the exosome-mediated miRNA transfer but not an induction of miR-105's endogenous expression in the recipient cells, as its level in exosome-treated cells was not significantly affected by an RNA polymerase II inhibitor (Figure 2E). When we treated HMVECs with PKH67-labeled exosomes secreted by MDA-MB-231 cells that were transfected with Cy3-labeled miR-105, the Cy3 fluorescence was observed in >90% of recipient cells where it largely colocalized with the PKH67 lipid dye that labeled the exosomal membranes (Figure S1D). In contrast, no internalization of naked Cy3-labeled miR-105 was observed in HMVECs (Figure S1D).

Cancer-secreted miR-105 downregulates tight junctions and destroys the barrier function of endothelial monolayers

We next examined the miR-105 regulation of the putative target ZO-1, a central molecular component of tight junctions (TJs) which comprise a major group of cell-cell adhesion complexes in endothelial and epithelial cells. The four predicted miR-105 binding sites in the 3′UTR of human ZO-1 were cloned into a reporter plasmid and assessed for their responsiveness to miR-105 in HMVECs. Site I and site II, which are conserved among most species, responded to retrovirus-expressed miR-105 by directing a 50–65% reduction in reporter gene expression, whereas the other two sites did not. When both sites I and II were

present downstream of reporter gene, a greater reduction in gene expression was observed (Figure S2A).

Consistent with the results from the reporter assay, ectopic expression of miR-105, or treatment with exosomes derived from the MDA-MB-231 (high-miR-105) but not the MCF-10A cells (low-miR-105), resulted in a significant decrease of ZO-1 expression at both mRNA and protein levels in HMVECs (Figure 3A–C). The effect of MDA-MB-231 exosomes could be abolished by transfecting the recipient cells with miR-105 inhibitor (Figure 3B–C). It was unlikely to require additional exosomal components that are unique to MDA-MB-231, as exosomes secreted by MCF-10A cells stably overexpressing and secreting miR-105 (Figure S2B) and by other high-miR-105 BC cells but not by low-miR-105 BC cells (Figure 2A–B) also downregulated ZO-1 expression in recipient HMVECs (Figures 3C & S2C). When HMVEC monolayers were analyzed by immunofluorescence, those treated with high-miR-105 exosomes (secreted by MCF10A/miR-105 and MDA-MB-231) exhibited marked reduction of ZO-1 and internalization of another TJ protein occludin from cell junctions, whereas the junctional level of VE-cadherin was not significantly affected (Figure 3D).

We next performed an *in vitro* permeability assay by measuring the traversing of rhodamine-labeled M_r 70K dextran probes through HMVEC monolayers growing on 0.4-μm filters. Similar to the effect induced by VEGF, treatment of the endothelial barrier with MDA-MB-231 exosomes also induced passage of the fluorescent probes from top to the bottom wells in a manner that was dependent on functional miR-105 and downregulation of ZO-1 (Figure 3E). When the trans-endothelial electrical resistance was measured in HMVEC monolayers, treatment with MDA-MB-231 exosomes significantly reduced the unit area resistance compared to PBS or MCF-10A exosome treatment. Inhibition of miR-105 and restored expression of ZO-1 in recipient HMVECs both abolished the effect of MBC-derived exosomes (Figure 3F). The effect of miR-105-containing exosomes on vascular destruction was further tested in a 3D vascular sprouting assay. In this system, endothelial cells formed vascular sprouts after 4 to 5 days in culture. At this time, purified exosomes from MCF10A/vec (control) or MCF10A/miR-105 cells were added into the culture media, and the effects on already established vascular structures were analyzed 5 days later. We observed a clear and significant destruction of vascular structures with the treatment of miR-105-containing exosomes (from MCF10A/miR-105) compared to the control (Figure 3G). Consistent with these results, ectopic expression of miR-105 or treatment with MBC exosomes significantly induced migration in HMVECs through the miR-105/ZO-1-mediated mechanism (Figure 3H). Lastly, to directly simulate the barrier-traversing step in metastasis, trans-endothelial invasion of cancer cells was examined using HMVEC monolayers grown on 3-μm filters. The number of GFP-labeled MDA-231-HM cells that had invaded through HMVECs treated with MDA-MB-231 exosomes was significantly greater compared to those invaded through untreated or MCF-10A exosome-treated HMVECs, and both miR-105 inhibition and ZO-1 restoration in recipient cells interfered with this effect (Figure 3I).

Cancer-secreted miR-105 induces vascular permeability and promotes metastasis *in vivo*

To further demonstrate the *in vivo* effect of exosomal miR-105 on endothelial barriers, we injected exosomes secreted by MCF10A/vec (low-miR-105), MCF10A/miR-105 (high-miR-105), or MDA-MB-231 cells (high-miR-105), or PBS as control, into the tail vein of NOD/SCID/IL2Rγ-null (NSG) mice and examined lung and brain, organs that frequently host BC metastases, after exosome treatment. The results indicated that exosomes with high-miR-105, but not those with low-miR-105, significantly increased miR-105 levels in lung and brain (Figure 4A), accompanied by reduced ZO-1 expression in $CD31^+$ endothelial cells (Figure 4B) and enhanced vascular permeability (Figures 4C & S3). In another experiment, mice were pretreated with exosomes secreted by MCF-10A or MDA-MB-231 cells (or PBS as control) before an intracardiac injection of luciferase-labeled MDA-MB-231 cells. Three weeks later, tissues were collected for RT-qPCR of luciferase gene using mouse 18S as internal control to quantify metastases. Consistent with their effect on destroying the endothelial barriers, MDA-MB-231, but not MCF-10A exosomes significantly increased metastases in lung and brain (Figure 4D).

MiR-105 overexpression in poorly metastatic BC cells promotes metastasis *in vivo*

To determine if the miR-105 level in primary tumors regulates endothelial barriers and metastasis, we stably overexpressed miR-105 in an MCF-10A-derived tumorigenic line MCFDCIS, which forms comedo ductal carcinoma *in situ*-like lesions that spontaneously progress to invasive tumors (Hu et al., 2008; Miller et al., 2000). Compared to vector-transduced control cells, the miR-105-overexpressing MCFDCIS cells also secreted a higher level of miR-105 (Figure S4A), and showed reduced ZO-1 protein expression and significantly enhanced migration in transwell and wound closure assays (Figure S4B–D). Restoration of ZO-1 using an overexpressing plasmid that lacks the 3′UTR abolished the pro-migratory effect of miR-105. We next established orthotopic xenografts using luciferase-labeled MCFDCIS cells with or without miR-105 overexpression. Although miR-105 did not seem to affect primary tumor growth (Figure S4E–F), distant metastases were significantly induced in lung and brain in mice bearing miR-105-overexpressing tumors at week 6 (Figure 5A–B). Histological staining indicated that in contrast to the MCFDCIS/vec tumors showing moderate local invasiveness, MCFDCIS/miR-105 tumors displayed no clear margin and extensively infiltrated into the surrounding tissues (Figure 5C). In addition, the *in vivo* vascular permeability in lung, liver, and brain of mice bearing miR-105-overexpressing tumors was dramatically increased compared to the control group (Figures 5D & S4H), whereas a relatively high vascular permeability was observed in the primary tumors of both groups (Figure S4G–H). In mice bearing miR-105-overexpressing tumors, miR-105 was detected not only in primary tumors but also in the metastasis-free areas of distant organs (Figure 5E). Reduced level of ZO-1 was observed in the $CD31^+$ vascular endothelial cells in the lung and brain of mice with high-miR-105 xenografts (Figure 5F). These results collectively suggest that tumor cells expressing and consequently secreting higher level of miR-105 acquire greater metastatic potential through the dual advantages of enhanced tumor cell invasion and weakened endothelial barriers in the host.

MiR-105 inhibition suppresses metastasis and restores vascular integrity *in vivo*

To further explore the potential therapeutic effect of miR-105 intervention, we established xenografts from high-miR-105, high-metastatic MDA-231-HM cells that were generated through explant culture of a spontaneous meningeal metastasis of MDA-MB-231. *In vitro* treatment of these cells with an anti-miR-105 compound increased ZO-1 expression and suppressed migration (Figure S5A–B), consistent with the effect of miR-105 observed in other experiments. *In vivo* treatment with the anti-miR-105 compound reduced the volume of primary tumors and suppressed distant metastases to lung and brain compared to the groups receiving PBS or control compound (Figure 6A–C). Tumors treated with anti-miR-105 had a clear margin with significantly reduced tumor cell infiltration into the surrounding tissues (Figure 6D). Although Ki-67 staining did not show a significant difference among the tumor groups, anti-miR-105-treated tumors showed a higher level of ZO-1 and a higher percentage of apoptotic cells, as indicated by cleaved caspase-3 (Figure 6E). The *in vivo* vascular permeability assay indicated lack of rhodamine-dextran penetration into various tissues in tumor-free mice; conversely, leakage of the dye into these tissues in tumor-bearing animals occurred even at a pre-metastatic stage (Figures 6F & S5C), which suggests an effect of tumor-secreted factors in destroying the vascular integrity of a distant organ during early pre-metastatic niche formation. Notably, treatment with anti-miR-105 efficiently blocked this effect, restoring the vascular integrity in tumor-bearing animals (Figures 6F & S5C). Restored ZO-1 expression in $CD31^+$ vascular endothelial cells was observed in the lung and brain of tumor-bearing mice treated with anti-miR-105 compound (Figure 6G). Thus, anti-miR-105 treatment suppresses metastasis by reducing tumor invasiveness and restoring the barrier function of endothelial niche cells.

MiR-105 is associated with ZO-1 expression and metastatic progression in BC

Because miR-105 is uniquely expressed and secreted by MBC cells, it is possible that cancer-secreted miR-105 can be detected in the circulation of BC patients, where miR-105 may serve as a prognostic marker for metastatic potential. To explore this, we first measured the serum miRNA levels in mice bearing MDA-231-HM xenograft tumors at either pre-metastatic (week 3 after cancer cell implantation) or metastatic stages (week 6 after cancer cell implantation) in comparison to tumor-free animals. Circulating miR-105, but not two other miRNAs (miR-155 and miR-375), was significantly elevated in tumor-bearing animals at both pre- and metastatic stages (Figure 7A), suggesting that miR-105 derived from primary tumors with high miR-105 levels and high metastatic potential can be detected in the blood at an early stage before clinical detection of metastasis. We next compared the serum miRNA levels among 38 stage II–III BC patients. By comparing miRNA levels in circulating exosomes and the corresponding exosome-depleted serum fraction, we found that circulating miR-105 and miR-181a predominantly existed in exosomes, whereas two other miRNAs (miR-375 and miR-422b) were detected in both exosomes and exosome-depleted fraction at comparable levels (Figure S6). In circulating exosomes purified from sera, levels of miR-105, but not two other miRNAs (miR-181a and miR-375), were significantly higher in patients who later developed distant metastases during the 4.2 years of mean follow-up (n = 16) than those who did not (n = 22) (Figure 7B). To further determine if circulating miR-105 in BC patients are functionally active in regulating endothelial cells, we treated

established 3D vascular structures with serum from a healthy donor or a BC patient with a high level of circulating miR-105. The patient serum but not normal serum resulted in a destruction of vascular structures, which was abolished by the anti-miR-105 compound (Figure 7C).

In patients with paired serum and tumor specimens, we further detected a strong positive correlation between circulating (exosomal) and tumor miR-105 levels ($r = 0.85$, $p < 0.01$). In contrast, significant inverse correlations were detected between tumor miR-105 and ZO-1 ($r = -0.48$, $p = 0.03$), as well as between circulating (exosomal) miR-105 and tumor-adjacent vascular ZO-1 expression ($r = -0.49$, $p = 0.04$) (Figure 7D&F). These observations are consistent with the role of miR-105 in downregulating ZO-1. In addition, higher levels of tumor miR-105 and lower levels of tumor and vascular ZO-1 were observed in patients who later developed distant metastases compared to those who did not and to normal mammary tissues (Figure 7E–F), thus supporting the functional association of these genes with cancer metastasis. In a BC tissue array, significantly higher miR-105 and lower ZO-1 levels were detected in the primary tumors with distant or lymph node metastases ($n = 15$) compared to those without ($n = 60$), and the inverse correlation between miR-105 and ZO-1 remained significant among all cases ($r = -0.24$, $p = 0.04$) (Figure 7G). Overall, our clinical data suggest that cancer-derived miR-105 can serve as a blood-based marker for the prediction or early diagnosis of BC metastasis, and may play a role in promoting cancer progression by targeting ZO-1.

DISCUSSION

Exchange of cellular materials between cells through various paracrine and endocrine mechanisms is an important means of intercellular communication and can be mediated by exosomes. The tumor-derived adaptation of endothelial cells by miR-105 occurs during early pre-metastatic niche formation. Enhanced vascular permeability could then enhance cancer cell dissemination and growth at distant sites through multiple means, including: i) plasma protein leakage that results in enhanced entrapment and hence concentration of tumor cells; ii) enhanced dissemination of tumor cells to distant sites resulting in autocrine signaling that overwhelms any inhibitory signaling at the distant site; and iii) additional exosome cargos and/or plasma proteins that leak into secondary organs and alter cellular physiology towards a pro-metastatic/tumor-supportive phenotype. In fact, vascular destabilization at the pre-metastatic lung niche has been previously described and involves a synergistic effect among angiopoietin 2, matrix metalloproteinase (MMP) 3, and MMP10 (Huang et al., 2009). Thus, therapies targeting miR-105 and these protein factors, in combination with existing conventional therapies, may serve as an effective treatment for cancer patients with a high risk of metastasis (e.g., indicated by high levels of circulating miR-105). Understanding mechanisms leading to miR-105 overexpression in MBC, which is an ongoing direction in our lab, may reveal additional strategies for miR-105 intervention.

Downregulation or loss of TJs, frequently as a result of reduced expression of TJ-associated proteins, contributes to cancer progression by altering cell migration, proliferation, polarity, and differentiation (Brennan et al., 2010; Georgiadis et al., 2010; Itoh and Bissell, 2003; Martin and Jiang, 2009). Reduction of TJ-associated ZO-1 in primary breast tumors due to

decreased expression or cytoplasmic localization is associated with metastasis in BC patients (Martin et al., 2004; Polette et al., 2005). Our study identifies miR-105 as a key regulator of ZO-1, suggesting one mechanism of TJ disruption associated with cancer progression and metastasis. The Rho family of small GTPases has been implicated in the regulation and function of TJs (Connolly et al., 2002; Gonzalez-Mariscal et al., 2008; Jou et al., 1998; Shen et al., 2006). The Rho-associated protein kinase, a downstream effector of RhoA, regulates acto-myosin contractility, TJ assembly, and endothelial capillary formation through phosphorylation of the regulatory myosin light chain (MLC2). Relevant to our story, junctional proteins including ZO-1 have been reported to regulate Rho GTPases through interacting with guanine nucleotide exchange factors and GTPase activating proteins (Citi et al., 2011). In our study, overexpression of miR-105 or treatment with exosomes carrying miR-105 did not alter the activity of RhoA, Rac1/2/3, or Cdc42, or the phosphorylation of MLC2, in recipient HMVECs (data not shown), suggesting that the small GTPases are not downstream effectors of the herein identified miR-105/ZO-1 pathway. In endothelial cells that normally express low miR-105 levels (data not shown), ectopic, cancer-derived miR-105 transferred via exosomes can effectively reduce ZO-1 expression and disrupt the barrier function of these cells both *in vitro* and *in vivo*. Although miR-105 secreted by the primary tumor may only affect a fraction of endothelial niche cells, this would be sufficient to open “gates” in these natural monolayer barriers for traversal of cancer cells thereby facilitating metastasis. In addition, contact-dependent intercellular miRNA transfer between two adjacent cells through the transmembrane channel protein SIDT1 has recently been reported (Elhassan et al., 2012). Through this pathway, cancer-derived miRNAs (e.g., miR-105) that are transferred to a distant organ via circulating exosomes may further extend their regulatory effect to those interconnected niche cells without direct exosome uptake. In patients with familial hypercholesterolemia but not normal subjects, circulating miR-105 can be detected on high-density lipoprotein which delivers the miRNA to recipient cells as an exosome-independent mechanism (Vickers et al., 2011). It would be interesting to determine the non-cancer source of circulating miR-105 and its role in regulating vascular permeability through the herein demonstrated pathway in these patients.

It is likely that additional target genes and pathways regulated by miR-105 also contribute to its pro-metastatic effect. Although overexpression of miR-105 in MCFDCIS xenografts did not significantly affect primary tumor growth, anti-miR-105 treatment in animals bearing MDA-231-HM xenografts reduced tumor volume and induced apoptosis of tumor cells. This may suggest a cancer- or/and niche-specific effect of miR-105 that facilitates cancer cell survival and therefore, promotes metastasis. Interestingly, miR-105 has been reported as a tumor suppressor that inhibits proliferation through downregulating CDK6 in prostate cancer cells (Honeywell et al., 2013). This miRNA may also have an anti-inflammatory effect in gingival keratinocytes through targeting TLR-2 (Benakanakere et al., 2009). In several cancer cell lines of non-breast origin, mature miR-105 is undetectable, possibly due to the nuclear retention of miR-105 precursors (Lee et al., 2008). These suggest important tissue-specific mechanisms controlling the biogenesis and function of miR-105. Understanding these mechanisms and their relevance to cancer progression and metastasis will provide further rationales for targeting miR-105 as a treatment for MBC.

MiRNA transfer between cancer cells and the genetically normal niche cells is apparently bidirectional. In addition to the cancer-derived adaptation of niche cells, normal epithelial cells also secrete and transfer anti-proliferative miRNAs (e.g., miR-143) to cancer cells, as a potential strategy to maintain tissue homeostasis at an early stage in cancer formation (Kosaka et al., 2012). In contrast, exosomes secreted by stromal fibroblasts promote BC cell protrusion and motility through Wnt-planar cell polarity signaling (Luga et al., 2012). Because exosomes are secreted by multiple types of normal cells and mediate their natural functions such as antigen presentation (Thery et al., 2002), targeting exosome secretion as a potential means of blocking this mode of cancer–host crosstalk requires identification of cancer-specific molecules/pathways that control exosome production. The recently reported high expression of Rab27A in cancer and the effect of Rab27A interference by reducing exosome production in multiple melanoma cell lines may provide an approach to specifically inhibit cancer-derived exosomes (Peinado et al., 2012). In addition, as the exosomal secretion of miRNAs exhibits a highly selective pattern that differs between cancer and normal cells (Table S1) (Pigati et al., 2010), understanding the cellular selection mechanism for miRNA secretion which may involve RNA-binding proteins recognizing the primary or secondary structures of miRNAs and its dysregulation in cancer may reveal unique strategies to block cancer-specific miRNA secretion. Lastly, characterization of cancer-secreted messengers and effectors, such as miR-105, will enable selection of patients for the corresponding targeted therapy and eventually combination therapy simultaneously targeting multiple secretory miRNAs and/or proteins. Such patient selection may be achieved by a quantitative blood test for circulating miR-105, which correlates with metastasis in early-stage BC patients. In developing personalized diagnostics and therapeutics, a combination of miR-105 with other miRNA and/or protein markers in the blood which would better specify the disease traits at the individual level will likely enhance our ability to select BC patients with a high risk of metastasis for preventive treatment that targets miR-105 and other effectors.

EXPERIMENTAL PROCEDURES

Clinical specimens

Human specimens were obtained from voluntarily consenting patients at the City of Hope Medical Center (Duarte, CA) under institutional review board-approved protocols. The clinical information is summarized in Tables S2–5. Details can be found in Supplemental Information.

Cells, plasmids and viruses

Please see Supplemental Information.

Exosome purification and electron microscopy (EM)

Detailed protocols for preparing exosomes by ultracentrifugation can be found in Supplemental Information. For EM, exosomes were fixed with 2% paraformaldehyde, loaded on 200-mesh Formvar-coated grids, and then contrasted and embedded as described in (Thery et al., 2006). Solexa deep sequencing of exosomal and cellular RNA and genome-

wide interrogation were performed as described (Wu et al., 2012); datasets were submitted to GEO (GSE50429).

RNA extraction, RT-qPCR, Western blot analysis, and immunofluorescence (IF)

These procedures were performed as described previously (Tsuyada et al., 2012; Wang et al., 2011; Yu et al., 2010). See Supplemental Information for details.

Trans-endothelial electrical resistance (TEER), endothelial permeability, and 3D vascular sprouting assays

Detailed protocols can be found in Supplemental Information. Vascular sprouting assay was performed as described using microcarrier-beads coated with endothelial cells and embedded in 3D fibrin gel (Newman et al., 2011).

Wound closure, transwell migration, and trans-endothelial invasion assays

Wound closure and transwell migration assays were performed as previously described (Wang et al., 2006). Detailed protocols for trans-endothelial invasion assay can be found in Supplemental Information.

Animals

All animal experiments were approved by the institutional animal care and use committee at City of Hope. Detailed procedures can be found in Supplemental Information. The control and miR-105 targeted compounds used in the miR-105 intervention study had the same chemical modification pattern, chimeric 2′-fluoro and 2′-methoxyethyl modifications on a phosphorothioate backbone (Davis et al., 2006) and were synthesized at Regulus Therapeutics (San Diego, CA). The same compounds were also used *in vitro* to transfect MDA-231-HM cells in Figure S5A&B.

In situ hybridization (ISH) and immunohistochemistry (IHC)

Please see Supplemental Information.

Statistical analyses

All results were confirmed in at least three independent experiments, and data from one representative experiment was shown. All quantitative data are presented as mean ± standard deviation (SD). The statistical analysis was performed using SAS 9.2 software package. Student *t* tests were used for comparison of means of quantitative data between groups. The correlations between serum and tumor miR-105 and between miR-105 and ZO-1 expression were evaluated by Pearson correlation coefficient (r). Values of $p < 0.05$ were considered significant.

Supplementary Material

Refer to Web version on PubMed Central for supplementary material.

Acknowledgments

This work was supported by the City of Hope Women's Cancer Program, National Institutes of Health (NIH)/ National Cancer Institute (NCI) grants R01CA166020 (SEW) and R01CA163586 (SEW), California Breast Cancer Research Program grant 17IB-0054 (SEW), Breast Cancer Research Foundation-American Association for Cancer Research grant 12-60-26-WANG (SEW), and National Key Basic Research Development Program (973 Program) of China No. 2012CB9333004 (XR). Research reported in this publication included work performed in Core facilities supported by the NIH/NCI under grant number P30CA33572. We thank the Center for Cancer Research, NCI for funding support to PCL. We acknowledge Dr. Alan Fanning for kindly providing the ZO-1 plasmid. We also thank Drs. John Rossi, Hua Yu, John Shively, Linda Malkas, Andrew Raubitschek, Ren-Jang Lin, Michael Barish, Susan Kane, Shiuan Chen, and Joanne Mortimer for valuable comments, as well as the City of Hope Core Facilities for highly professional services. GS had grant support from Celgene. EGM was a full-time employee of a company developing miRNA therapeutics, Regulus Therapeutics.

References

Arroyo JD, Chevillet JR, Kroh EM, Ruf IK, Pritchard CC, Gibson DF, Mitchell PS, Bennett CF, Pogosova-Agadjanyan EL, Stirewalt DL, et al. Argonaute2 complexes carry a population of circulating microRNAs independent of vesicles in human plasma. Proc Natl Acad Sci U S A. 2011; 108:5003–5008. [PubMed: 21383194]

Benakanakere MR, Li Q, Eskan MA, Singh AV, Zhao J, Galicia JC, Stathopoulou P, Knudsen TB, Kinane DF. Modulation of TLR2 protein expression by miR-105 in human oral keratinocytes. J Biol Chem. 2009; 284:23107–23115. [PubMed: 19509287]

Brennan K, Offiah G, McSherry EA, Hopkins AM. Tight junctions: a barrier to the initiation and progression of breast cancer? J Biomed Biotechnol. 2010; 2010:460607. [PubMed: 19920867]

Calin GA, Croce CM. MicroRNA signatures in human cancers. Nat Rev Cancer. 2006; 6:857–866. [PubMed: 17060945]

Chambers AF, Groom AC, MacDonald IC. Dissemination and growth of cancer cells in metastatic sites. Nat Rev Cancer. 2002; 2:563–572. [PubMed: 12154349]

Citi S, Spadaro D, Schneider Y, Stutz J, Pulimeno P. Regulation of small GTPases at epithelial cell-cell junctions. Mol Membr Biol. 2011; 28:427–444. [PubMed: 21781017]

Connolly JO, Simpson N, Hewlett L, Hall A. Rac regulates endothelial morphogenesis and capillary assembly. Mol Biol Cell. 2002; 13:2474–2485. [PubMed: 12134084]

Davis S, Lollo B, Freier S, Esau C. Improved targeting of miRNA with antisense oligonucleotides. Nucleic Acids Res. 2006; 34:2294–2304. [PubMed: 16690972]

Elhassan MO, Christie J, Duxbury MS. Homo sapiens systemic RNA interference-defective-1 transmembrane family member 1 (SIDT1) protein mediates contact-dependent small RNA transfer and microRNA-21-driven chemoresistance. J Biol Chem. 2012; 287:5267–5277. [PubMed: 22174421]

Fabbri M, Paone A, Calore F, Galli R, Gaudio E, Santhanam R, Lovat F, Fadda P, Mao C, Nuovo GJ, et al. MicroRNAs bind to Toll-like receptors to induce prometastatic inflammatory response. Proc Natl Acad Sci U S A. 2012; 109:E2110–2116. [PubMed: 22753494]

Georgiadis A, Tschernutter M, Bainbridge JW, Balaggan KS, Mowat F, West EL, Munro PM, Thrasher AJ, Matter K, Balda MS, Ali RR. The tight junction associated signalling proteins ZO-1 and ZONAB regulate retinal pigment epithelium homeostasis in mice. PLoS One. 2010; 5:e15730. [PubMed: 21209887]

Gonzalez-Mariscal L, Tapia R, Chamorro D. Crosstalk of tight junction components with signaling pathways. Biochim Biophys Acta. 2008; 1778:729–756. [PubMed: 17950242]

Heneghan HM, Miller N, Lowery AJ, Sweeney KJ, Newell J, Kerin MJ. Circulating microRNAs as novel minimally invasive biomarkers for breast cancer. Ann Surg. 2010; 251:499–505. [PubMed: 20134314]

Honeywell DR, Cabrita MA, Zhao H, Dimitroulakos J, Addison CL. miR-105 Inhibits Prostate Tumour Growth by Suppressing CDK6 Levels. PLoS One. 2013; 8:e70515. [PubMed: 23950948]

Hood JL, San RS, Wickline SA. Exosomes released by melanoma cells prepare sentinel lymph nodes for tumor metastasis. Cancer Res. 2011; 71:3792–3801. [PubMed: 21478294]

Hu M, Yao J, Carroll DK, Weremowicz S, Chen H, Carrasco D, Richardson A, Violette S, Nikolskaya T, Nikolsky Y, et al. Regulation of in situ to invasive breast carcinoma transition. Cancer Cell. 2008; 13:394–406. [PubMed: 18455123]

Huang Y, Song N, Ding Y, Yuan S, Li X, Cai H, Shi H, Luo Y. Pulmonary vascular destabilization in the premetastatic phase facilitates lung metastasis. Cancer Res. 2009; 69:7529–7537. [PubMed: 19773447]

Iorio MV, Ferracin M, Liu CG, Veronese A, Spizzo R, Sabbioni S, Magri E, Pedriali M, Fabbri M, Campiglio M, et al. MicroRNA gene expression deregulation in human breast cancer. Cancer Res. 2005; 65:7065–7070. [PubMed: 16103053]

Itoh M, Bissell MJ. The organization of tight junctions in epithelia: implications for mammary gland biology and breast tumorigenesis. J Mammary Gland Biol Neoplasia. 2003; 8:449–462. [PubMed: 14985640]

Jou TS, Schneeberger EE, Nelson WJ. Structural and functional regulation of tight junctions by RhoA and Rac1 small GTPases. J Cell Biol. 1998; 142:101–115. [PubMed: 9660866]

Jung EJ, Santarpia L, Kim J, Esteva FJ, Moretti E, Buzdar AU, Di Leo A, Le XF, Bast RC Jr, Park ST, et al. Plasma microRNA 210 levels correlate with sensitivity to trastuzumab and tumor presence in breast cancer patients. Cancer. 2012; 118:2603–2614. [PubMed: 22370716]

Kaplan RN, Riba RD, Zacharoulis S, Bramley AH, Vincent L, Costa C, MacDonald DD, Jin DK, Shido K, Kerns SA, et al. VEGFR1-positive haematopoietic bone marrow progenitors initiate the pre-metastatic niche. Nature. 2005; 438:820–827. [PubMed: 16341007]

Kosaka N, Iguchi H, Yoshioka Y, Hagiwara K, Takeshita F, Ochiya T. Competitive interactions of cancer cells and normal cells via secretory microRNAs. J Biol Chem. 2012; 287:1397–1405. [PubMed: 22123823]

Lee EJ, Baek M, Gusev Y, Brackett DJ, Nuovo GJ, Schmittgen TD. Systematic evaluation of microRNA processing patterns in tissues, cell lines, and tumors. RNA. 2008; 14:35–42. [PubMed: 18025253]

Luga V, Zhang L, Viloria-Petit AM, Ogunjimi AA, Inanlou MR, Chiu E, Buchanan M, Hosein AN, Basik M, Wrana JL. Exosomes mediate stromal mobilization of autocrine Wnt-PCP signaling in breast cancer cell migration. Cell. 2012; 151:1542–1556. [PubMed: 23260141]

Martin TA, Jiang WG. Loss of tight junction barrier function and its role in cancer metastasis. Biochim Biophys Acta. 2009; 1788:872–891. [PubMed: 19059202]

Martin TA, Watkins G, Mansel RE, Jiang WG. Loss of tight junction plaque molecules in breast cancer tissues is associated with a poor prognosis in patients with breast cancer. Eur J Cancer. 2004; 40:2717–2725. [PubMed: 15571953]

Miller FR, Santner SJ, Tait L, Dawson PJ. MCF10DCIS.com xenograft model of human comedo ductal carcinoma in situ. J Natl Cancer Inst. 2000; 92:1185–1186. [PubMed: 10904098]

Mitchell PS, Parkin RK, Kroh EM, Fritz BR, Wyman SK, Pogosova-Agadjanyan EL, Peterson A, Noteboom J, O'Briant KC, Allen A, et al. Circulating microRNAs as stable blood-based markers for cancer detection. Proc Natl Acad Sci U S A. 2008; 105:10513–10518. [PubMed: 18663219]

Newman AC, Nakatsu MN, Chou W, Gershon PD, Hughes CC. The requirement for fibroblasts in angiogenesis: fibroblast-derived matrix proteins are essential for endothelial cell lumen formation. Mol Biol Cell. 2011; 22:3791–3800. [PubMed: 21865599]

Nicolini A, Giardino R, Carpi A, Ferrari P, Anselmi L, Colosimo S, Conte M, Fini M, Giavaresi G, Berti P, Miccoli P. Metastatic breast cancer: an updating. Biomed Pharmacother. 2006; 60:548–556. [PubMed: 16950593]

Paget S. The distribution of secondary growths in cancer of the breast. Lancet. 1889; 133:571–573.

Peinado H, Aleckovic M, Lavotshkin S, Matei I, Costa-Silva B, Moreno-Bueno G, Hergueta-Redondo M, Williams C, Garcia-Santos G, Ghajar C, et al. Melanoma exosomes educate bone marrow progenitor cells toward a pro-metastatic phenotype through MET. Nat Med. 2012; 18:883–891. [PubMed: 22635005]

Pigati L, Yaddanapudi SC, Iyengar R, Kim DJ, Hearn SA, Danforth D, Hastings ML, Duelli DM. Selective release of microRNA species from normal and malignant mammary epithelial cells. PLoS One. 2010; 5:e13515. [PubMed: 20976003]

Podsypanina K, Du YC, Jechlinger M, Beverly LJ, Hambardzumyan D, Varmus H. Seeding and propagation of untransformed mouse mammary cells in the lung. Science. 2008; 321:1841–1844. [PubMed: 18755941]

Polette M, Gilles C, Nawrocki-Raby B, Lohi J, Hunziker W, Foidart JM, Birembaut P. Membrane-type 1 matrix metalloproteinase expression is regulated by zonula occludens-1 in human breast cancer cells. Cancer Res. 2005; 65:7691–7698. [PubMed: 16140936]

Psaila B, Lyden D. The metastatic niche: adapting the foreign soil. Nat Rev Cancer. 2009; 9:285–293. [PubMed: 19308068]

Redis RS, Calin S, Yang Y, You MJ, Calin GA. Cell-to-cell miRNA transfer: from body homeostasis to therapy. Pharmacol Ther. 2012; 136:169–174. [PubMed: 22903157]

Roth C, Rack B, Muller V, Janni W, Pantel K, Schwarzenbach H. Circulating microRNAs as blood-based markers for patients with primary and metastatic breast cancer. Breast Cancer Res. 2010; 12:R90. [PubMed: 21047409]

Rubens RD. 7. Management of advanced breast cancer. Int J Clin Pract. 2001; 55:676–679. [PubMed: 11777292]

Sethi N, Kang Y. Unravelling the complexity of metastasis - molecular understanding and targeted therapies. Nat Rev Cancer. 2011; 11:735–748. [PubMed: 21941285]

Shen L, Black ED, Witkowski ED, Lencer WI, Guerriero V, Schneeberger EE, Turner JR. Myosin light chain phosphorylation regulates barrier function by remodeling tight junction structure. J Cell Sci. 2006; 119:2095–2106. [PubMed: 16638813]

Skog J, Wurdinger T, van Rijn S, Meijer DH, Gainche L, Sena-Esteves M, Curry WT Jr, Carter BS, Krichevsky AM, Breakefield XO. Glioblastoma microvesicles transport RNA and proteins that promote tumour growth and provide diagnostic biomarkers. Nat Cell Biol. 2008; 10:1470–1476. [PubMed: 19011622]

Taylor DD, Gercel-Taylor C. MicroRNA signatures of tumor-derived exosomes as diagnostic biomarkers of ovarian cancer. Gynecol Oncol. 2008; 110:13–21. [PubMed: 18589210]

Thery C, Amigorena S, Raposo G, Clayton A. Isolation and characterization of exosomes from cell culture supernatants and biological fluids. Curr Protoc Cell Biol. 2006; Chapter 3(Unit 3):22. [PubMed: 18228490]

Thery C, Zitvogel L, Amigorena S. Exosomes: composition, biogenesis and function. Nat Rev Immunol. 2002; 2:569–579. [PubMed: 12154376]

Tsuyada A, Chow A, Wu J, Somlo G, Chu P, Loera S, Luu T, Li AX, Wu X, Ye W, et al. CCL2 mediates cross-talk between cancer cells and stromal fibroblasts that regulates breast cancer stem cells. Cancer Res. 2012; 72:2768–2779. [PubMed: 22472119]

Turchinovich A, Weiz L, Langheinz A, Burwinkel B. Characterization of extracellular circulating microRNA. Nucleic Acids Res. 2011; 39:7223–7233. [PubMed: 21609964]

Valadi H, Ekstrom K, Bossios A, Sjostrand M, Lee JJ, Lotvall JO. Exosome-mediated transfer of mRNAs and microRNAs is a novel mechanism of genetic exchange between cells. Nat Cell Biol. 2007; 9:654–659. [PubMed: 17486113]

Vickers KC, Palmisano BT, Shoucri BM, Shamburek RD, Remaley AT. MicroRNAs are transported in plasma and delivered to recipient cells by high-density lipoproteins. Nat Cell Biol. 2011; 13:423–433. [PubMed: 21423178]

Vickers KC, Remaley AT. Lipid-based carriers of microRNAs and intercellular communication. Curr Opin Lipidol. 2012; 23:91–97. [PubMed: 22418571]

Wang SE, Narasanna A, Perez-Torres M, Xiang B, Wu FY, Yang S, Carpenter G, Gazdar AF, Muthuswamy SK, Arteaga CL. HER2 kinase domain mutation results in constitutive phosphorylation and activation of HER2 and EGFR and resistance to EGFR tyrosine kinase inhibitors. Cancer Cell. 2006; 10:25–38. [PubMed: 16843263]

Wang Y, Yu Y, Tsuyada A, Ren X, Wu X, Stubblefield K, Rankin-Gee EK, Wang SE. Transforming growth factor-beta regulates the sphere-initiating stem cell-like feature in breast cancer through miRNA-181 and ATM. Oncogene. 2011; 30:1470–1480. [PubMed: 21102523]

Wu X, Somlo G, Yu Y, Palomares MR, Li AX, Zhou W, Chow A, Yen Y, Rossi JJ, Gao H, et al. De novo sequencing of circulating miRNAs identifies novel markers predicting clinical outcome of locally advanced breast cancer. J Transl Med. 2012; 10:42. [PubMed: 22400902]

Yardley DA. Visceral disease in patients with metastatic breast cancer: efficacy and safety of treatment with ixabepilone and other chemotherapeutic agents. Clin Breast Cancer. 2010; 10:64–73. [PubMed: 20133261]

Yu Y, Wang Y, Ren X, Tsuyada A, Li X, Liu LJ, Wang SE. Context-dependent bidirectional regulation of the mutS homolog 2 by transforming growth factor {beta} contributes to chemoresistance in breast cancer cells. Mol Cancer Res. 2010; 8:1633–1642. [PubMed: 21047769]

Yuan A, Farber EL, Rapoport AL, Tejada D, Deniskin R, Akhmedov NB, Farber DB. Transfer of microRNAs by embryonic stem cell microvesicles. PLoS One. 2009; 4:e4722. [PubMed: 19266099]

Zhang Y, Liu D, Chen X, Li J, Li L, Bian Z, Sun F, Lu J, Yin Y, Cai X, et al. Secreted monocytic miR-150 enhances targeted endothelial cell migration. Mol Cell. 2010; 39:133–144. [PubMed: 20603081]

Zhu W, Qin W, Atasoy U, Sauter ER. Circulating microRNAs in breast cancer and healthy subjects. BMC Res Notes. 2009; 2:89. [PubMed: 19454029]

Zhuang G, Wu X, Jiang Z, Kasman I, Yao J, Guan Y, Oeh J, Modrusan Z, Bais C, Sampath D, Ferrara N. Tumour-secreted miR-9 promotes endothelial cell migration and angiogenesis by activating the JAK-STAT pathway. EMBO J. 2012; 31:3513–3523. [PubMed: 22773185]

SIGNIFICANCE

In this study, we set out to identify cancer-secreted miRNAs that participate in cancer metastasis by adapting the niche cells. Our results demonstrate an important role of miR-105 in destroying the vascular endothelial barriers in the host during early pre-metastatic niche formation by targeting the cellular tight junctions. In breast cancer patients, increased levels of miR-105 in the circulation can be detected at the pre-metastatic stage and correlate with the occurrence of metastasis. Anti-miR-105 treatment suppresses metastasis and abolishes the systemic effect of tumor-derived miR-105 on niche adaptation. Therefore, these observations strongly suggest clinical applications of miR-105 as a predictive or early-diagnostic blood-borne marker as well as a therapeutic target for breast cancer metastasis.

HIGHLIGHTS

- MiR-105 is uniquely expressed and secreted by metastatic breast cancer cells.
- MiR-105 directly targets the tight junction protein ZO-1.
- Cancer-secreted miR-105 destroys endothelial barriers in the host.
- Circulating miR-105 predicts metastasis in early-stage breast cancer patients.

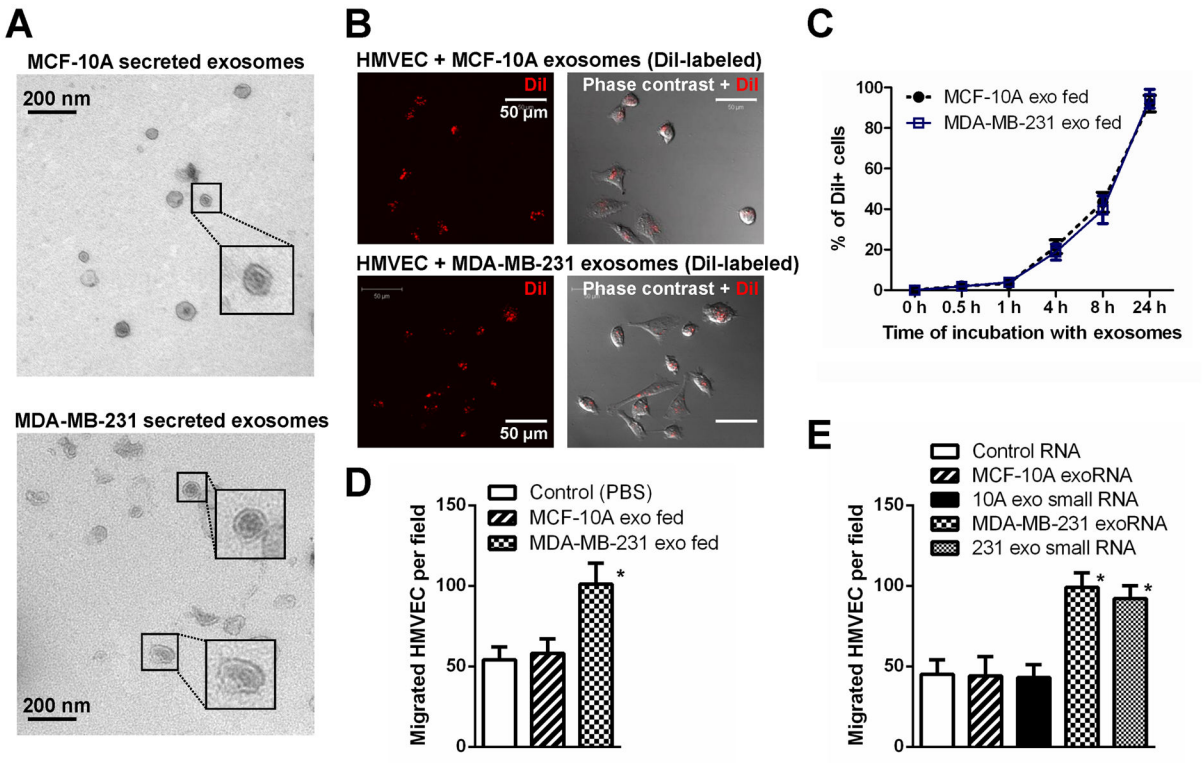

Figure 1. MBC-secreted exosomal RNA regulates migration of endothelial cells

(A) EM images of exosomes secreted by MCF-10A and MDA-MB-231 cells. **(B)** Primary HMVECs were incubated with DiI-labeled exosomes (red) for 24 hr before fluorescent and phase contrast images were captured. **(C)** HMVECs incubated with DiI-labeled exosomes for indicated time were analyzed by flow cytometry for DiI uptake. **(D)** After 48 hr incubation with exosomes or PBS (as control), HMVECs were analyzed for transwell migration and cells that had migrated within 8 hr were quantified from triplicate wells. **(E)** HMVECs transfected with equal amount of total or small (<200 nt) RNA extracted from MCF-10A or MDA-MB-231 (abbreviated to MDA-231 or 231 in Figures) secreted exosomes, or control RNA (cel-miR-67), were subjected to transwell migration at 48 hr post transfection. *$p < 0.005$ compared to control group. Results are presented as mean ± SD.

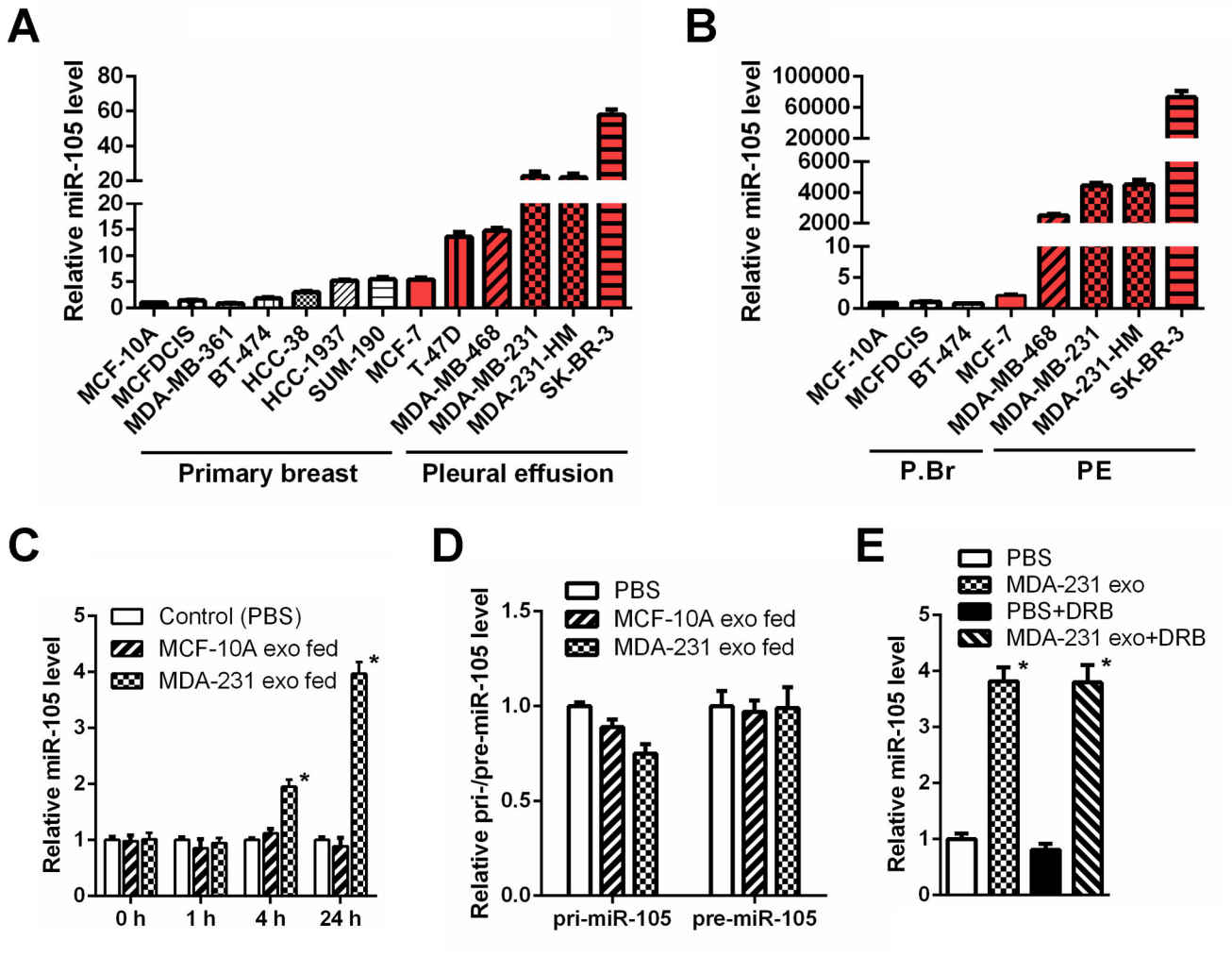

Figure 2. MiR-105 is specifically expressed and secreted by MBC cells and can be transferred to endothelial cells via exosome secretion

Cellular **(A)** and exosomal **(B)** RNA were extracted from various breast cell lines and subjected to miR-105 RT-qPCR. Data was normalized to levels of U6 (cellular; **A**) or miR-16 (exosomal; **B**), and compared to the non-tumor line MCF-10A. MBC lines originally isolated from pleural effusion are indicated by red columns. **(C)** RNA was extracted from HMVECs incubated with exosomes of different origins for indicated time and analyzed for miR-105 level using U6 as internal control. At each time point, data was compared to PBS-treated cells. **(D)** RNA extracted from HMVECs incubated with exosomes of different origins for 24 hr (or PBS as control) was analyzed for the level of pri-miR-105 or pre-miR-105. **(E)** MDA-MB-231-secreted exosomes were fed to HMVECs in the presence or absence of DRB (20 μM). After 24 hr, RNA extracted from the recipient cells was analyzed for miR-105 level. *$p < 0.005$ compared to PBS treatment. Results are presented as mean ± SD. (See also Figure S1 and Table S1.)

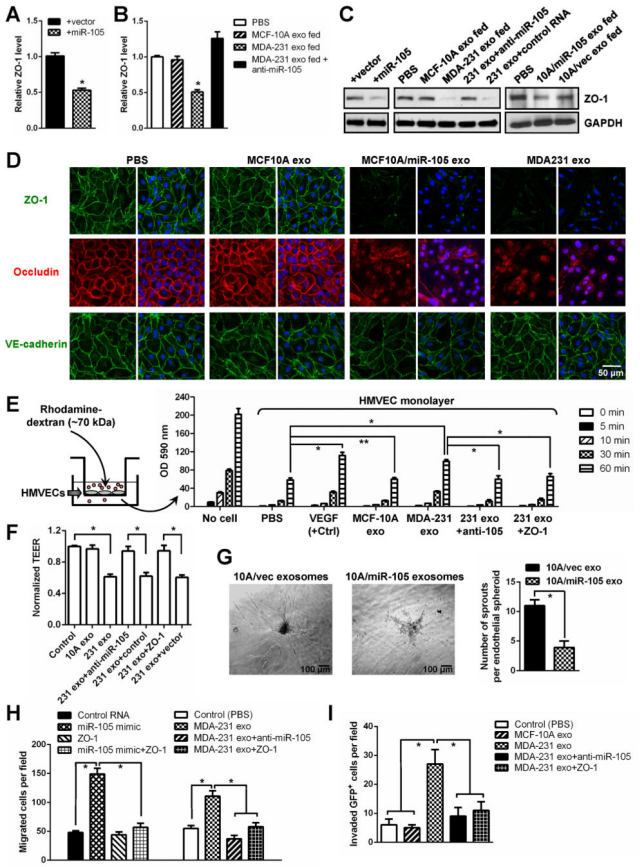

Figure 3. Cancer-secreted miR-105 downregulates tight junctions and destroys the barrier function of endothelial monolayer

(A) HMVECs transduced with miR-105 or vector were analyzed for ZO-1 expression by RT-qPCR. **(B)** HMVECs treated as indicated were analyzed for the RNA level of ZO-1. **(C)** HMVECs treated as indicated were analyzed by Western blot. **(D)** HMVEC monolayers were treated as indicated for 48 hr and analyzed by IF for ZO-1 (green), occludin (red) and VE-cadherin (green). DAPI (blue): cell nuclei. **(E)** The permeability of treated HMVEC monolayers grown on 0.4-μm filters was measured by the appearance of rhodamine-dextran, which was added to the top well at the beginning of the experiment, in the bottom well during a 1 hr time course. The absorbance at 590 nm at each time point was indicated. Treatment of the HMVEC monolayer with VEGF (50 ng/ml) for 8 hr was included as a positive control to show cytokine-induced permeability. The absorbance at the 1 hr time point was compared to the PBS (control) condition. *$p < 0.005$. **$p > 0.05$. **(F)** HMVEC monolayers grown on filters and treated as indicated were analyzed for TEER. Calculated unit area resistance from triplicate wells was normalized to the control (PBS) treatment. **(G)** Treatment with miR-105-containing exosomes resulted in a vascular destruction. Vascular sprouting assay was established for 5 days, at which time 1 μg of purified exosomes from MCF10A/vec (control) or MCF10A/miR-105 cells were added into the culture media. Vascular structures were imaged 5 days after the treatment, and representative images were shown (left panel). Vascular sprouts per spheroid were counted and graphed (right panel). At least 50 spheroids were counted in each experiment and the experiment was repeated three

times. *p < 0.05. **(H)** HMVECs treated as indicated were subjected to transwell migration. Cells that had migrated within 8 hr were quantified from triplicate wells. *p < 0.005. **(I)** HMVEC monolayers grown on 3-μm filters were treated as indicated before GFP-labeled MDA-231-HM cells were seeded in the transwell inserts. After 10 hr, the GFP^+ cells on the bottom side of filters were quantified under a fluorescent microscope. *p < 0.005. Results are presented as mean ± SD. (See also Figure S2.)

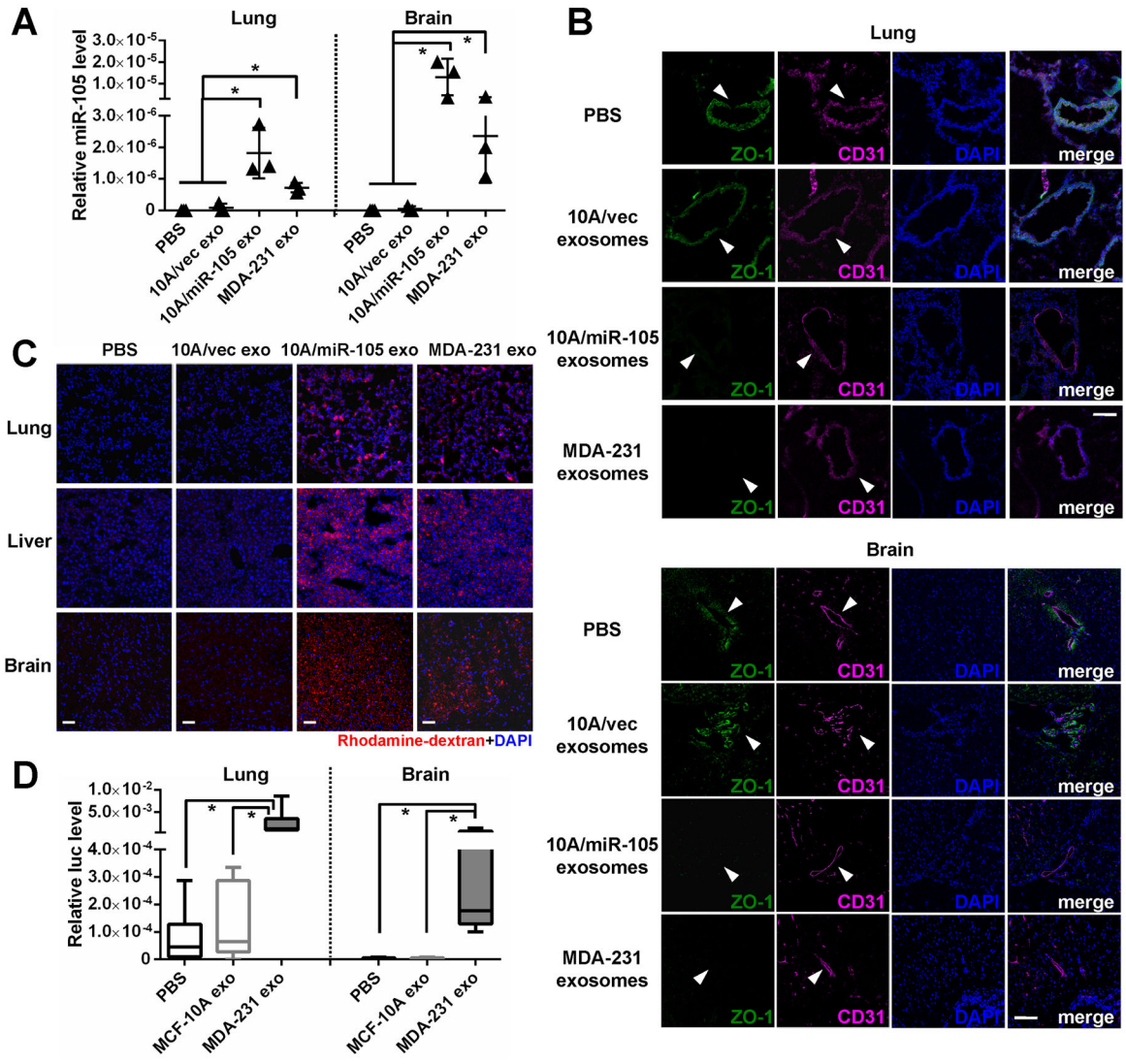

Figure 4. Cancer-secreted miR-105 induces vascular permeability and promotes metastasis *in vivo*

(A) Exosomes secreted by MCF10A/vec, MCF10A/miR-105, or MDA-MB-231 cells, or PBS (as control), were intravenously injected into the tail vein of NSG mice (n = 3) twice a week. After 5 injections, tissues were collected for RT-qPCR of miR-105 using U6 as internal control. *p < 0.05. **(B)** Collected lung and brain tissues were subjected to double-label IF for ZO-1 (green) and CD31 (pink). Structures positive for CD31 are indicated by arrowheads. Bar = 100 μm. **(C)** *In vivo* vascular permeability determined by the appearance of intravenously injected rhodamine-dextran (red) (n = 3). Representative images are shown. DAPI (blue): cell nuclei. Bar = 100 μm. **(D)** Exosomes secreted by MCF-10A or MDA-MB-231 cells, or PBS (as control), were intravenously injected into the tail vein of NSG mice (n = 6) twice a week. After 5 injections, all mice received intracardiac injection of luciferase-labeled MDA-MB-231 cells. Three weeks later, tissues were collected for RT-qPCR of luciferase gene using mouse 18S as internal control to quantify metastases. *p < 0.05. Results are presented as mean ± SD. (See also Figure S3.)

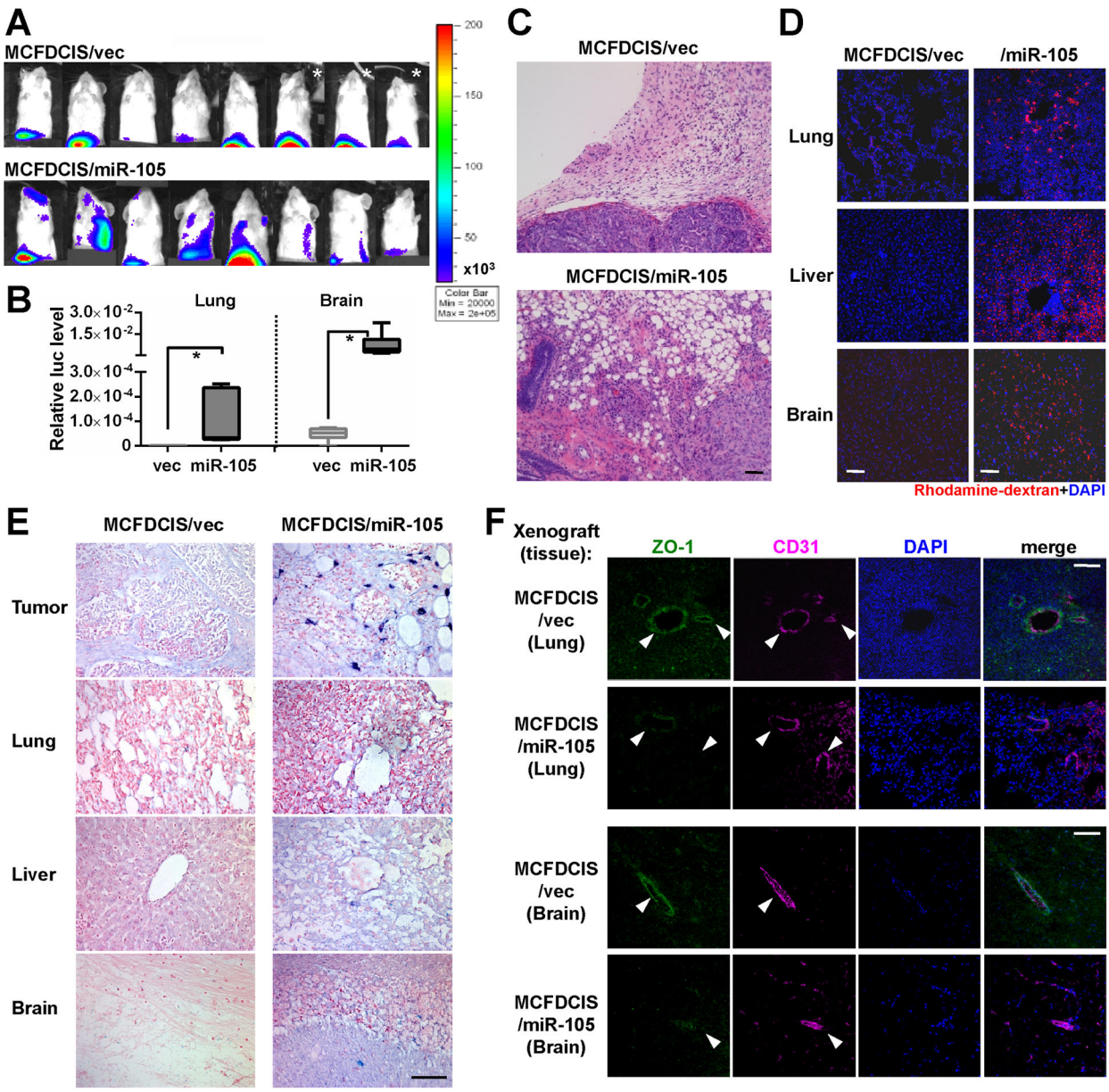

Figure 5. MiR-105 overexpression in poorly metastatic BC cells promotes metastasis *in vivo*

(A) Luciferase-labeled MCFDCIS/vec or MCFDCIS/miR-105 cells were injected into the No. 4 mammary fat pad of NSG mice (n = 8). BLI at week 6 was shown. *Due to the extensive tumor burden these 3 mice were sacrificed at week 5.5; their images at week 5 were shown. **(B)** Quantification of metastases in lung and brain. Mice shown in **A** were sacrificed at week 6 and tissues were subjected to RT-qPCR of luciferase gene using mouse 18S as internal control (n = 8). Results are presented as mean ± SD. *$p < 0.05$. **(C)** Representative H&E images of the tumor edges showing local invasiveness. Bar = 50 μm. **(D)** *In vivo* vascular permeability determined by the appearance of intravenously injected rhodamine-dextran (red) in various organs. Tissues were collected from mice bearing MCFDCIS/vec or MCFDCIS/miR-105 xenografts (n = 3) that were sacrificed at week 6.

Representative images are shown. DAPI (blue): cell nuclei. Bar = 100 μm. **(E)** Representative images of miR-105 ISH in tissues collected from the two groups. Bar = 50 μm. **(F)** Collected tissues were subjected to double-label IF for ZO-1 (green) and CD31 (pink). Structures positive for CD31 are indicated by arrowheads. Bar = 100 μm. (See also Figure S4.)

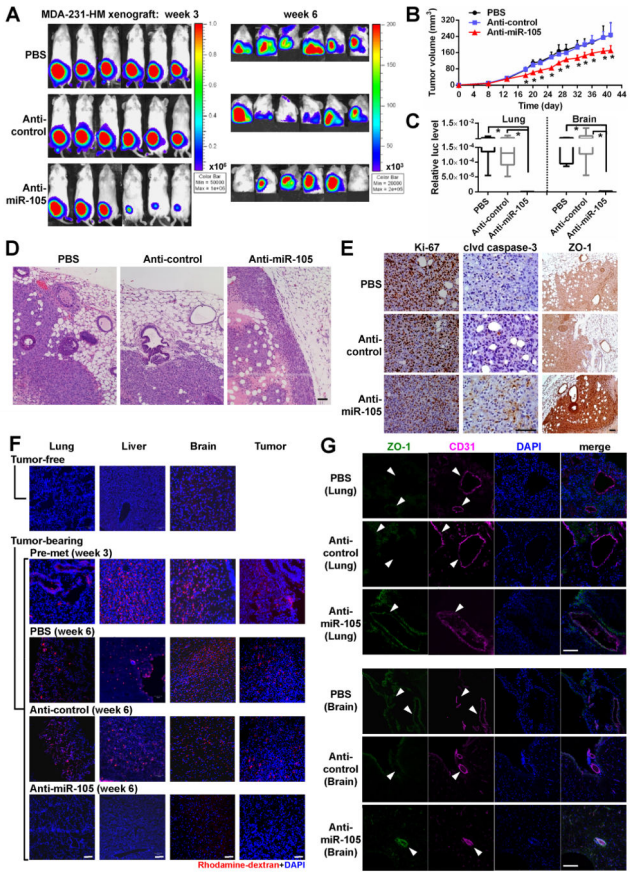

Figure 6. MiR-105 inhibition suppresses metastasis and restores vascular integrity *in vivo*

(A) Luciferase-labeled MDA-231-HM cells were injected into the No. 4 mammary fat pad of NSG mice. Mice were divided into 3 groups (n = 6) for treatment with PBS, anti-miR-105 compound, or control compound. BLI at week 3 and week 6 were shown. **(B)** Tumor volume determined in the 3 groups. *p < 0.005 comparing to the other 2 groups. **(C)** Quantification of metastases in lung and brain. Mice shown in **A** were sacrificed at week 6 and tissues were subjected to RT-qPCR of luciferase gene using mouse 18S as internal control (n = 6). *p < 0.01. **(D)** Representative H&E images of the tumor edges showing local invasiveness. Bar = 50 μm. **(E)** IHC was performed in xenograft tumors using antibodies of Ki-67, cleaved caspase-3 and ZO-1. Representative images are shown. Bar = 50 μm. **(F)** *In vivo* vascular permeability indicated by the penetration of rhodamine-dextran (red) into various organs. Tissues were collected from tumor-free NSG mice as well as mice bearing MDA-231-HM tumors that were untreated when sacrificed at week 3 after tumor cell implantation (the pre-metastatic group) or treated as indicated and sacrificed at week 6 (n = 4). Representative images are shown. DAPI (blue): cell nuclei. Bar = 100 μm. **(G)** Tissues were subjected to double-label IF for ZO-1 (green) and CD31 (pink). Structures positive for CD31 are indicated by arrowheads. Bar = 100 μm. Results are presented as mean ± SD. (See also Figure S5.)

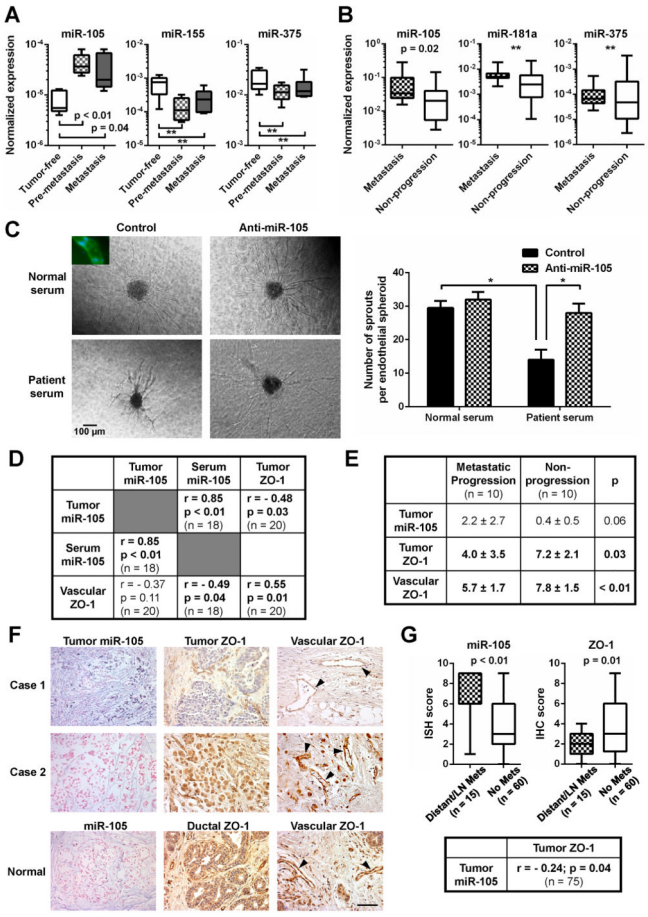

Figure 7. MiR-105 is associated with ZO-1 expression and metastatic progression in BC

(A) MiRNA levels in the sera of tumor-free or MDA-231-HM tumor-bearing mice (Pre-metastasis: serum collected at week 3; Metastasis: serum collected at week 6; n = 5–6) were measured by RT-qPCR and normalized to miR-16. **p > 0.05. **(B)** Circulating exosomes were isolated from serum samples of stage II–III BC patients. MiRNAs were measured by RT-qPCR, normalized to miR-16, and compared among patients who developed distant metastases during the follow up (n = 16) and those who did not (n = 22). **p > 0.05. **(C)** Circulating miR-105 in patient serum resulted in a vascular destruction. Vascular structures established from HMVECs that were transfected with anti-miR-105 compound or control compound were treated with human serum from a healthy donor or a BC patient with a high level of circulating miR-105. Representative images of the treated vascular structures were shown (left panel). Inset: structures were stained with CD31 antibody (green) and DAPI (blue). Vascular sprouts per spheroid were counted and graphed (right panel). At least 50 spheroids were counted in each experiment and the experiment was repeated three times. *p < 0.05. **(D)** Correlation analyses of tumor miR-105, serum (exosomal) miR-105, and ZO-1 levels in BC patients. MiR-105 levels in tumor cells and ZO-1 levels in tumor cells (tumor ZO-1) or tumor-adjacent vascular structures (vascular ZO-1) were determined by ISH and IHC, respectively, and scored as described in Experimental Procedures. Serum (exosomal) miR-105 levels were determined by PCR using miR-16 as a normalizer. Correlation

analyses were carried out between two sets of quantified data as indicated. Pearson correlation coefficient (*R*) and *p* value are shown. **(E)** The scores of tumor miR-105, tumor ZO-1, and vascular ZO-1 staining were compared between stage II–III BC patients who developed distant metastases (n = 10) and those who did not (n = 10). Mean and SD of the staining scores in each group are shown. **(F)** Representative images of miR-105 and ZO-1 staining in tumor and normal breast tissue sections. Vascular structures are indicated by arrowheads. Bar = 100 μm. **(G)** Levels of tumor miR-105 and ZO-1 determined in a BC tissue array. The ISH or IHC scores were compared between primary tumors with distant or lymph node metastases (n = 15) and those without (n = 60). The correlation between miR-105 and ZO-1 was analyzed among all cases (n = 75). Results are presented as mean ± SD. (See also Figure S6 and Tables S2-5.)